

Prompt-Matched Semantic Segmentation

Lingbo Liu¹ Jianlong Chang² Bruce X.B. Yu¹ Liang Lin³ Qi Tian² Chang-Wen Chen¹

¹The Hong Kong Polytechnic University, Hong Kong

²Huawei Cloud & AI, Shenzhen 518000, China ³Sun Yat-Sen University, China

Abstract

The objective of this work is to explore how to effectively and efficiently adapt pre-trained visual foundation models to various downstream tasks of semantic segmentation. Previous methods usually fine-tuned the entire networks for each specific dataset, which will be burdensome to store massive parameters of these networks. A few recent works attempted to insert some extra trainable parameters into the frozen networks to learn visual prompts for parameter-efficient tuning. However, these works showed poor generality as they were designed specifically for Transformers. Moreover, using limited information in these schemes, they exhibited a poor capacity to learn beneficial prompts. To alleviate these issues, we propose a novel Stage-wise Prompt-Matched Framework for generic and effective visual prompt tuning. Specifically, to ensure generality, we divide the pre-trained backbone with frozen parameters into multiple stages and perform prompt learning between different stages, which makes the proposed scheme applicable to various architectures of CNN and Transformer. For effective tuning, a lightweight Semantic-aware Prompt Matcher (SPM) is designed to progressively learn reasonable prompts with a recurrent mechanism, guided by the rich information of interim semantic maps. Working as deep matched filter of representation learning, the proposed SPM can well transform the output of the previous stage into a desirable input for the next stage, thus achieving the better matching/stimulating for the pre-trained knowledge. Extensive experiments on four benchmarks demonstrate that the proposed scheme can achieve a promising trade-off between parameter efficiency and performance effectiveness. Our code and models will be released.

1. Introduction

Semantic segmentation [42] is a fundamental yet challenging visual problem in computer vision, which aims to automatically perform pixel-level labeling with a set of object categories for the given image. Over the past decades, this problem has attracted extensive research in industry and

academia, since it can facilitate a variety of downstream applications, e.g., scene understanding [40], satellite image analysis [37], and medical auxiliary diagnosis [23].

In the literature, various Convolutional Neural Networks (CNN) and Transformer architectures have been proposed for this problem [3, 14, 19, 29, 34, 39, 46, 50, 52]. Instead of learning from scratch [60], most previous works usually first acquired a foundation model pre-trained on large-scale benchmarks (e.g., ImageNet [12]), and then fine-tuned the network’s parameters on specific downstream datasets. There are usually two strategies for model fine-tuning. The first one is **Full-Tuning** [2] that adjusts all parameters of the whole network. However, it usually requires large amounts of training data with rich annotations for effective representation learning. Moreover, this strategy requires storing a proprietary model with massive parameters for each downstream task/dataset, which is burdensome and unsustainable for many service platforms. The second strategy is **Head-Tuning** [15], which freezes the parameters of the backbone network and only optimizes the model’s head. Intuitively, all tasks share the same backbone and we only need to maintain an individual head for each task. Despite being parameter efficient, this strategy has a limited capacity to learn discriminative features and can not well exploit pre-trained knowledge for complex visual understanding. Overall, the above strategies suffer from various issues, and we desire a more effective and efficient fine-tuning method for widespread downstream tasks of semantic segmentation.

Recently, **Prompt-Tuning** [38] has been proposed to explore the knowledge of frozen language models by inserting textual prompts into the downstream input. Inspired by its great success in natural language processing (NLP), a few works [9, 31] in the field of computer vision have attempted to introduce some trainable prompt parameters to energize the pre-trained knowledge in those parameter-frozen visual foundation models. Despite certain progress, these works suffered from the following issues. **First**, they were specially designed for Transformer, not generic to commonly-used CNN architectures. For instance, VPT [31] learned visual prompts in the token space, while AdaptFormer [9] replaced the original MLP block with a parallel bottleneck

module. **Second**, these works modified the original structure of every foundation unit. In practice, the different stages of foundation models with standard structures are usually compressed and embedded into high-speed inference devices [41, 49]. However, extensive structural modifications make the above approaches not directly applicable on these devices. **Third**, these works learned visual prompts with limited information in a black-box mapping manner. Specifically, they only utilized the final recognition loss to optimize prompt parameters and had limited capacities to learn reasonable prompts. It is worth noting that image semantic segmentation is more challenging than image recognition, requiring richer information to perform pixel-wise inferences. Therefore, informative knowledge should be fully explored to generate beneficial visual prompts for parameter-efficient representation learning.

To address the above issues, we propose a novel Stage-wise Prompt-Matched Framework, which can effectively adapt those frozen foundation models of different architectures to facilitate semantic segmentation in various scenarios. Specifically, instead of modifying each foundation module with extra parameters, we partition the given backbone network into multiple stages and perform stage-wise prompt tuning for specific datasets. This makes our method applicable to various backbone architectures and those stage-wise embedded high-speed devices. Moreover, for effective and efficient tuning, we introduce a lightweight trainable module termed Semantic-aware Prompt Matcher (SPM) that incorporates rich information of interim semantic maps to learn reasonable visual prompts between any two stages in a progressive and recurrent manner. Working like deep matched filtering, our SPM can effectively transform the output representation of the previous stage into an appropriate input representation for the next stage, making it better to match/stimulate the pre-trained knowledge in the frozen backbone. Finally, we apply the proposed SPM to fine-tune various backbone networks such as ResNet [22] and Vision Transformer [16] to handle semantic segmentation of natural, satellite, and medical images. Extensive experiments conducted on four benchmarks show the parameter efficiency and performance effectiveness of the proposed method. In particular, optimizing only a small number of parameters of our SPM and the head segmenter, our method not only significantly outperforms existing parameter-efficient fine-tuning methods, but also is comparable or even better than *Full-Tuning*.

In summary, the contributions of our work are three-fold:

- A novel Stage-wise Prompt-Matched Framework is proposed to effectively and efficiently fine-tune those pre-trained foundation backbones with frozen parameters. Without specifically modifying the structure of foundation units, our method is universal for various network architectures of CNN and Transformer.
- A lightweight SPM is introduced to progressively learn reasonable visual prompts between different stages of the backbone through a recurrent mechanism. Guided by the rich information of interim semantic maps, our SPM can well transform the output of the previous stage into an appropriate input for the next stage, thus better energizing the pre-trained knowledge.
- Extensive experiments on four benchmarks demonstrate that our method is performance-effective and parameter-efficient for fine-tuning foundation models to various downstream tasks of semantic segmentation.

2. Related Work

Prompt Tuning: In recent years, various large-scale NLP models such as BERT [13], GPT-3 [5], and Pangu- α [54] have been developed by pre-training on huge datasets. With the emerging prompt tuning, these large-scale models achieved impressive transfer performance on myriads of downstream tasks such as translation [47], reading comprehension [27], question answering [51], etc. Inspired by the NLP prompt tuning paradigm, some computer vision researchers have attempted to facilitate visual understanding by fine-tuning vision-language models, where the textual prompts generated by text encoders were used to guide the representation learning of visual encoders [30, 43]. Despite achieving promising performance, these works relied heavily on the textual prompt design and can not be smoothly applied to various vision tasks. With this concern, a few recent works [9, 31] introduced some extra trainable parameters to directly learn visual prompts from the input visual features or randomized noise. Nevertheless, they were specially designed for Transforms and may fail to generate effective prompts due to the scarcity of instructive information. Therefore in this work, we are committed to exploring general and effective strategies for visual prompt tuning.

Semantic Segmentation: As a typical pixel-wise prediction problem, semantic segmentation has been significantly promoted by deep neural networks [10, 26, 28, 33, 35, 58]. For instance, [40] proposed Fully Convolutional Networks that replaced fully-connected layers with convolutional layers to handle images of arbitrary sizes. [45] applied a convolutional encoder-decoder architecture with skip connections to generate semantic maps with high resolutions. [56] used a backbone network to extract the feature maps of input images and then introduced a pyramid pooling module to aggregate different sub-region representations for multiscale contextual modeling. DeepLab family [7, 8] applied dilated convolutions to enlarge the network receptive fields and introduced Conditional Random Fields to refine the final segmentation results. Recently, Transformers [48] have also been applied to address this problem. One representative work is Segmenter [46], which divided

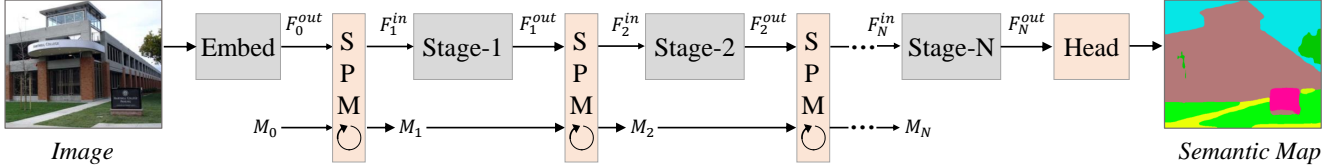


Figure 1. The architecture of our Stage-wise Prompt-Matched Framework for semantic segmentation prompt tuning. A lightweight Semantic-aware Prompt Matcher (SPM) is introduced to learn reasonable visual prompts recurrently between every two stages of the frozen backbone network. Guided by the rich information of interim semantic maps, the i -th SPM transforms the output feature F_{i-1}^{out} of the previous stage into a suitable input feature F_i^{in} for the next stage. M_i is the interim semantic map generated at the i -th SPM, while the initial map M_0 is generated from the statistic category probability of the training set. The symbol \odot denotes the recurrent prompt learning mechanism in our SPM. It is worth noting that only the parameters of our SPM and head segmenter are updated during the training phase.

the image into local patches and fed their linear embeddings into Vision Transformer [16] to capture global context at each layer for semantic segmentation. Despite progress, previous methods usually fine-tuned the parameters of the whole networks respectively for each specific task of semantic segmentation. It is burdensome to store massive parameters of these models, especially on some resource-constrained devices. Under this circumstance, we crave for a novel fine-tuning approach, where these tasks can share most of the parameters and achieve competitive results.

3. Methodology

3.1. Overall Architecture

In this work, we aim to utilize visual prompt learning to fine-tune the pre-trained foundation models for various downstream tasks, e.g., semantic segmentation. When developing our algorithm, we consider the following two questions: i) *where to learn visual prompts* and ii) *how to learn reasonable prompts*? We argue that previous works [9, 31] that performed customized prompt learning within each foundation unit are not applicable to different network architectures. We also observe that it is suboptimal to learn prompts with limited information of the final loss of the model’s head. So we desire an architecture-general prompt tuning model that fully exploits rich information to learn effective visual prompts.

To this end, we propose a unified Stage-wise Prompt-Matched Framework to effectively and efficiently fine-tune pre-trained foundation models to deal with downstream visual tasks. Here we take semantic segmentation as an example to illustrate the working process of our method. As shown in Figure 1, a semantic segmentation model usually consists of a universal backbone network pre-trained on a large-scale dataset and a customized head segmenter with random initialization. To reduce the number of tunable/stored parameters, we freeze the backbone network so that it can be shared by different tasks of semantic segmentation, while the head segmenter is optimized for each specific dataset. Inspired by previous NLP works [38], we apply prompt tuning to efficiently exploit the backbone

pre-trained knowledge to facilitate the visual representation learning of downstream semantic segmentation. To make our method applicable to various network architectures, we propose to learn visual prompts between different stages of the frozen backbone, without modifying the original structures of foundation units, e.g., residual module or transformer layer. Specifically, based on its architecture, we partition the backbone network into N stages, each of which is composed of multiple foundation units. Notice that there may be some embedding layers before the first stage. For convenience, the output feature of stage i is denoted as F_i^{out} ($i=1, \dots, N$), while the output feature of those embedding layers is denoted as F_0^{out} .

We then introduce a differentiable Semantic-aware Prompt Matcher (SPM) to learn visual prompts between two adjacent stages using a small number of parameters. As mentioned above, rich information is desired to perform prompt learning for various vision tasks including semantic segmentation. In this work, we find that interim semantic maps generated at intermediate layers can provide fine-grained prior information of object semantics distributions. Therefore, before stage i , our SPM incorporates the output feature F_{i-1}^{out} and the interim semantic map M_{i-1} of the previous stage to progressively learn reasonable visual prompts with a recurrent mechanism, since it is difficult to directly generate desirable prompts in some complex scenarios. After multiple iterations, we can obtain a refined semantic map M_i and a suitable input F_i^{in} for the stage i . This process can be formulated as:

$$F_i^{in}, M_i = SPM(F_{i-1}^{out}, M_{i-1}, R), \quad (1)$$

where R denotes the number of recurrent iterations. Notice that the initial semantic map M_0 is generated from the statistic category probability. More specifically, $M_0(x, y, c)$ at the position (x, y) is set to the pixel probability of the c -th category on the downstream training set. Intuitively, our SPM works as a representation-level matched filter that can better match the input features with the pre-trained knowledge in the backbone. More details of the proposed SPM are described in Section 3.2.

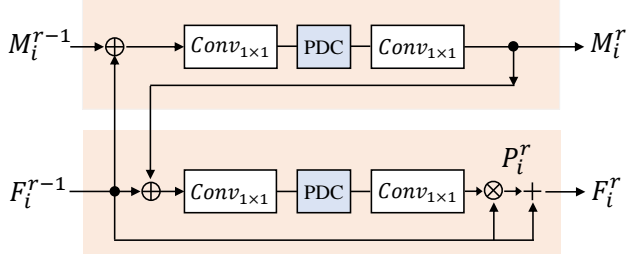


Figure 2. The architecture of Semantic-aware Prompt Matcher. $Conv_{1 \times 1}$ denotes a convolutional layer with a kernel size of 1×1 and PDC is our Pyramid Dilation Convolution in Figure 3. \oplus represents the feature concatenation operation, while \otimes denotes the element-wise multiplication.

As shown in Figure 1, our SPM is hierarchically inserted between different stages to learn semantic-aware visual prompts for downstream tasks. Finally, the output feature F_N^{out} of the N -th stage is fed into the head segmenter to generate the high-quality semantic map M .

3.2. Semantic-aware Prompt Matcher

In this subsection, we introduce the details of our SPM. The purpose of this module is to integrate rich information of interim semantic maps to learn reasonable visual prompts with a recurrent mechanism, so that the output feature of the previous stage can be transformed into a desirable input for the next stage. Specifically, before the stage i , our SPM first takes the feature F_{i-1}^{out} and the semantic map M_{i-1} to generate semantic-aware prompts. Similar to Recurrent Neural Networks [36], the prompted feature and the refined semantic map are fed back into SPM for recurrent prompt learning. Thus Eq.1 can be unfolded as follows:

$$\begin{aligned} F_i^0, M_i^0 &= F_{i-1}^{out}, M_{i-1}, \\ F_i^r, M_i^r &= f(F_i^{r-1}, M_i^{r-1}, \theta) \text{ for } r \text{ in } \{1, \dots, R\}, \\ F_i^{in}, M_i &= F_i^R, M_i^R, \end{aligned} \quad (2)$$

where $f(\cdot)$ denotes the SPM function with trainable parameters θ . F_i^r and M_i^r are the prompted feature and the refined semantic map at the r -th iteration of the i -th SPM. After R iterations, we can obtain the desirable input F_i^{in} for the next stage to better energize the pre-trained knowledge. Notice that θ is shared for all iterations for parameter efficiency.

Figure 2 shows the visual prompt tuning for the r -th iteration of the i -th SPM. We can see that our SPM consists of two parallel branches to refine the interim semantic map and generate the prompted feature. As mentioned in previous works [20, 61], long-range spatial context is crucial for semantic segmentation. Thus we develop a Pyramid Dilation Convolution (PDC) that uses four dilated group convolutional layers to capture the multi-scale lang-range context.

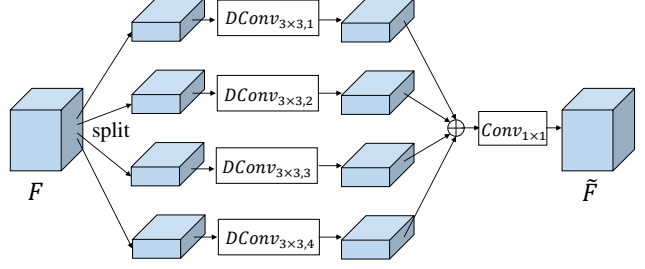


Figure 3. The architecture of Pyramid Dilation Convolution for long-range spatial context modeling. $DCConv_{3 \times 3, d}$ denotes a dilated group convolutional layer with a kernel size of 3×3 and a dilated rate of d . The input feature F and output feature \tilde{F} have the same dimension.

As shown in Figure 3, the input feature of PDC is divided into four sub-features along the channel dimension. The i -th sub-feature is fed into the i -th convolutional layer with a kernel size of 3×3 and a dilated rate of r . The outputs of all dilated layers are concatenated and fused using a 1×1 convolutional layer to restore the original channel number. The proposed PDC is integrated into both branches to generate the long-range contextualized features. The details of these branches are described as follows.

i) Interim Semantic Map Refinement: In this branch, we utilize the current feature to enhance the semantic map generated from the previous feature. Specifically, we first feed the concatenation of F_i^{r-1} and M_i^{r-1} into a 1×1 group convolutional layer to generate a compact feature $F_M^{i,r}$, which has a low channel number C for reducing the trainable parameters. We then apply the proposed PDC to obtain the long-range contextualized feature $\tilde{F}_M^{i,r}$, which is further fed into another 1×1 group convolutional layer to generate the refined semantic map M_i^r . This process can be formulated as:

$$\begin{aligned} F_M^{i,r} &= Conv_{1 \times 1}(F_i^{r-1} \oplus M_i^{r-1}), \\ \tilde{F}_M^{i,r} &= PDC(F_M^{i,r}), \\ M_i^r &= Softmax\{Conv_{1 \times 1}(\tilde{F}_M^{i,r})\}, \end{aligned} \quad (3)$$

where \oplus denotes the feature concatenation operation and the $Softmax$ layer is used to normalize the predicted scores of semantic categories at each location.

ii) Semantic-aware Prompt Generation: We then incorporate the feature F_i^{r-1} and the refined map M_i^r to learn visual prompts progressively. Similar to the first branch, we feed F_i^{r-1} and M_i^r into a 1×1 convolutional layer and a PDC to obtain the features $F_P^{i,r}$ and $\tilde{F}_P^{i,r}$. Inspired by the attention mechanism, we utilize another 1×1 convolutional layer to generate a prompt weight $W_P^{i,k}$, which is further applied to multiply with F_i^{k-1} to generate the visual prompt map P_i^k . Finally, F_i^{k-1} and P_i^k are added to obtain the new

prompted feature F_i^r . This process can be formulated as:

$$\begin{aligned} F_P^{i,r} &= \text{Conv}_{1 \times 1}(F_i^{r-1} \oplus M_i^r), \quad \tilde{F}_P^{i,r} = \text{PDC}(F_P^{i,r}), \\ W_P^{i,r} &= \text{Conv}_{1 \times 1}(\tilde{F}_P^{i,r}), \quad P_i^r = F_i^{r-1} \otimes W_P^{i,r}, \\ F_i^r &= F_i^{r-1} + P_i^r, \end{aligned} \quad (4)$$

where \otimes denotes the element-wise multiplication operation. Thanks to the progressive visual prompts generated by R iterations, we can effectively transform F_{i-1}^{out} to an appropriate F_i^{in} that can better stimulate the pre-trained knowledge in the i -th frozen stage of the backbone.

3.3. Network Optimization

During the training phase, the backbone network is frozen and we only update the parameters of our SPM and the head segmenter on downstream datasets. We utilize the Cross-Entropy (CE) loss function to optimize our network. The total loss is defined as follows:

$$\text{loss} = \text{CE}(M, \hat{M}) + \sum_{i=1}^N \sum_{k=1}^K a_i * \text{CE}(M_i^k, \hat{M}), \quad (5)$$

where \hat{M} is the ground-truth semantic map and M is our final semantic map predicted by the head segmenter. a_i is the loss weight of those interim semantic maps generated by the i -th SPM.

4. Experiment

4.1. Downstream Datasets

In this work, we conduct extensive experiments on five semantic segmentation datasets of various scenarios. Some examples of these datasets are visualized in Figure 4 and their details are described as follows.

ADE20K [59]: It is a large-scale scene parsing dataset with 150 types of objects and stuff. The public ADE20K consists of 20,210 images for training and 2,000 images for validation. These images have different resolutions and their objects suffer from great scale variations. This dataset is very challenging due to the high intra-class variances and low inter-class variances.

Vaihingen [1]: It is a medium-scale dataset for satellite image segmentation. This dataset consists of six types of semantic object, e.g., buildings, streets, cars, etc. The training set contains 344 images, while the testing set has 398 images. All images has the same resolution 512×512 .

CHASE-DB1 [17], STARE [24]: They are small-scale medical image segmentation datasets that aim to segment retinal vessels from background. CHASE-DB1 consists of 28 retinal images of multiethnic school children. STARE contains 20 retinal images of people of various ages, 10 of which have pathology. We follow [11] to preprocess these datasets and partition them for training/testing.

Table 1. Performance and the number of trainable parameters of different methods on the ADE20K dataset.

Method	Trainable Parameters (M)			mIoU \uparrow
	Backbone	Prompt	Head	
Full-Tuning [2]	42.41	0	25.54	43.96
Learn-from-Scratch [60]	42.41	0	25.54	34.84
Head-Tuning [15]	0	0	25.54	34.08
Bias-Tuning [53]	0.05	0	25.54	35.61
Side-Tuning [55]	0	6.51	25.54	36.42
Adapter [25]	0	6.80	25.54	37.22
Ours	0	3.11	25.54	41.83

4.2. Comparison with the Stage of the Art

In this subsection, we compare the proposed method with six basic and advanced methods, e.g., *Full-Tuning* [2], *Learn-from-Scratch* [60], *Head-Tuning* [15], *Bias-Tuning* [53], *Side-Tuning* [55] and *Adapter* [25]. The overall experimental settings are as follows:

Backbone Network: Here all methods adopt the popular ResNet-101 [22] network as backbone. Except *Learn-from-Scratch*, the backbone parameters of all methods were pre-trained with an auxiliary task of image recognition on the ImageNet-1K dataset [12]. The experiments of the Transformer backbone can be referred to Section 4.4.

Head Segmenter: For ADE20K and Vaihingen, all methods use Pyramid Pooling Module [56] as the head segmenter, since it has a great capacity to capture the scale variations of objects. On those medical datasets, the Progressive UPsampling head [57] is used, because retinal vessels are very thin and we require high-resolution segmentation results for medical diagnosis. Notice that all parameters of these heads are randomly initialized.

Trainable Parameters: During training, the head segmenter of each method is trainable. In addition, all methods except *Head-Tuning* will further optimize the whole/partial backbone network or introduce some prompt parameters. For instance, *Full-Tuning* and *Learn-from-Scratch* tune all backbone’s parameters, while *Bias-Tuning* tunes the bias of all layers in the backbone network. *Side-Tuning* introduces a side-network between the input and output of each residual module, while *Adapter* adds an adaptive-network on the output of the residual module. Both the side-network and adaptive-network are implemented by a 3×3 down-convolutional layer with 64 channels and 4 groups, and a 1×1 up-convolutional layer with the same number of channels as the output of the residual module. In our framework, the ResNet-101 backbone is divided into four stages, and the proposed SPM is inserted before each stage and the head segmenter to learn visual prompts hierarchically. The reduced channel C in SPM is uniformly set to 256 and the group number of convolutional layers in PDC is set to 16.

Training Details: In this work, we apply MMSegmentation [11] to implement our experiments on four Nvidia

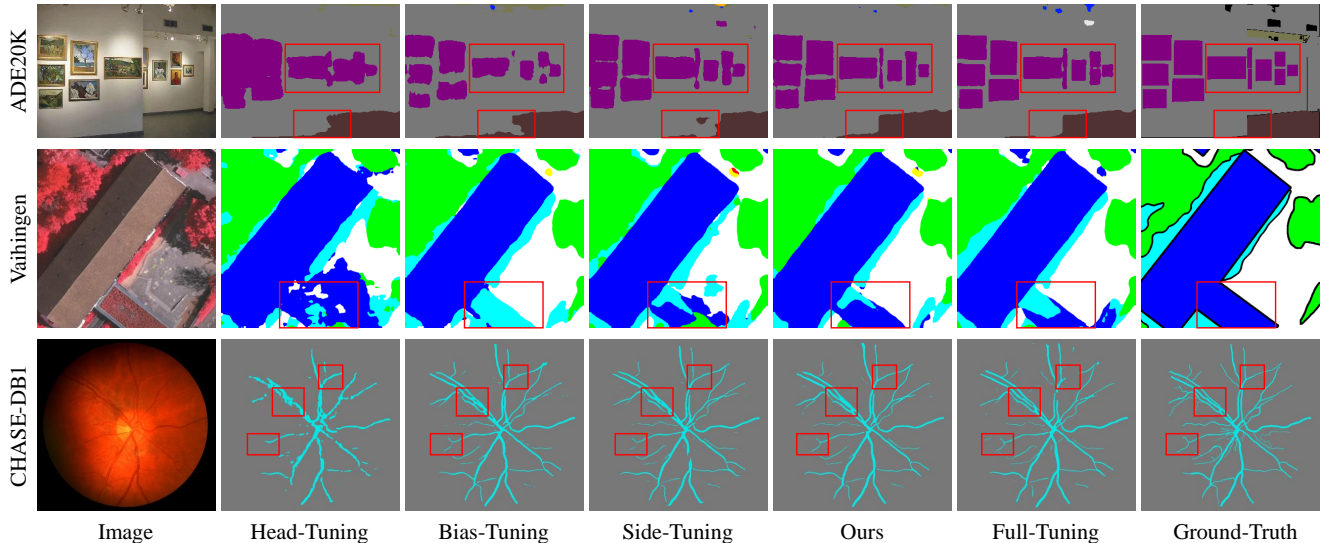


Figure 4. Visualization of various samples of semantic segmentation and the results of different methods. We observe that our method can generate high-quality semantic maps for natural, satellite, and medical image segmentation, especially in the regions of red boxes.

Table 2. Performance and the number of trainable parameters of different methods on the Vaihingen dataset.

Method	Trainable Parameters (M)			mIoU \uparrow
	Backbone	Prompt	Head	
Full-Tuning [2]	42.41	0	25.43	73.96
Learn-from-Scratch [60]	42.41	0	25.43	68.85
Head-Tuning [15]	0	0	25.43	62.45
Bias-Tuning [53]	0.05	0	25.43	68.06
Side-Tuning [55]	0	6.51	25.43	71.62
Adapter [25]	0	6.80	25.43	70.89
Ours	0	1.95	25.43	73.10

GeForce 3090 GPUs. On the ADE20K and Vaihingen datasets, those compared methods are trained for 80K iterations with a batch size of 16, while our method is trained with a batch size of 12 due to the GPU memory limitation and the number of training iterations is set to $80K \times 16 / 12 = 106K$. Therefore, all methods are optimized with the same epochs. For those medical datasets, all methods are trained for 8K iterations with a batch size of 4, due to the small amount of training data. The loss weight a_i in Eq.5 is set to $0.05/R$, $0.1/R$, $0.2/R$, $0.3/R$, and $0.4/R$ for the five stages, respectively

4.2.1 Large-scale Natural Image Segmentation

Table 1 summarizes the performance of different methods on the ADE20K dataset. We can observe that *Full-Tuning* achieves the best mIoU of 43.96%, significantly outperforming *Learn-from-Scratch* with the same number of trainable parameters, since the pre-trained backbone network contains rich prior knowledge. When the backbone

Table 3. The foreground Dice Similarity Coefficient (Dice) of one-shot medical image semantic segmentation.

Method	Trainable Parameters (M)			Dice \uparrow	
	Backbone	Prompt	Head	CHASE-DBI	STARE
Full-Tuning [2]	42.41	0	8.26	76.07 \pm 0.57	75.90 \pm 1.98
Learn from Scratch [60]	42.41	0	8.26	73.20 \pm 1.11	73.01 \pm 0.84
Head-Tuning [15]	0	0	8.26	59.35 \pm 0.55	54.14 \pm 1.82
Bias-Tuning [53]	0.05	0	8.26	75.83 \pm 0.68	74.70 \pm 1.11
Side-Tuning [55]	0	6.51	8.26	76.22 \pm 0.51	75.45 \pm 1.06
Adapter [25]	0	6.80	8.26	76.07 \pm 0.63	75.13 \pm 0.93
Ours	0	1.94	8.26	77.08\pm0.68	76.46\pm1.16

is frozen, *Head-Tuning* obtains a poor mIoU of 34.08%. With around 6M extra parameters, *Side-Tuning* and *Adapter* boost the mIoU to 36.42% and 37.22% respectively. In contrast, our method achieves a promising mIoU of 41.83%, using only 3.11M extra parameters to learn visual prompts between different frozen stages. In summary, the proposed method is better than all other parameter-efficient methods and also comparable to *Full-Tuning*. Moreover, Figure 4 also shows that our method can generate high-quality semantic maps for unconstrained natural scenarios.

4.2.2 Medium-scale Satellite Image Segmentation

Table 2 shows the performance of all methods on the Vaihingen dataset. We can observe that the compared results on this dataset are consistent with those on the ADE20K dataset. More specifically, *Head-Tuning* performs poorly when the backbone network is frozen. Without exception, *Side-Tuning* and *Adapter* are better than *Bias-Tuning*, but their results are still not satisfactory. In contrast, our method achieves a competitive mIoU of 73.10%, when using only 1.95M extra parameters for prompt learning. There is a

Table 4. Performance of different prompted stages and their number of prompt parameters (M) on three representative datasets. The recurrent number R of SPM is set to 1 in this experiment.

Stages	ADE20K		Vaihingen		CHASE-DB1	
	#Params	mIoU	#Params	mIoU	#Params	Dice
1	0.48	34.43	0.40	69.64	0.40	74.32±0.79
1-2	1.07	35.11	0.87	71.26	0.87	76.30±0.56
1-3	1.78	36.39	1.48	71.76	1.47	76.67±0.74
1-4	2.36	38.54	1.95	72.60	1.94	77.08±0.68
1-5	3.11	40.01	2.55	72.17	2.54	76.40±0.75

small gap between our method and *Full-Tuning* in terms of performance. What’s more, our method only needs to store a small number of parameters. This experiment shows the great potential of the proposed method for medium-scale satellite image segmentation.

4.2.3 One-shot Medical Image Segmentation

We further apply the proposed method to address one-shot medical semantic segmentation, since it is difficult and expensive to obtain massive medical images with pixel-wise annotations. Here we conduct five one-shot experiments. In each experiment, we randomly select a sample to train models and then validate them on the whole testing set. Table 3 shows the mean results and variances of different methods on two retinal segmentation datasets. We notice that those parameter-efficient fine-tuning methods are comparable to or even better than *Full-Tuning* under the one-shot setting, which is consistent with the findings [5, 54] in the NLP field. In particular, our method can achieve the best results on both datasets by learning visual prompts effectively with only 1.95M extra trainable parameters. The above experiments show the generalization of our method for semantic segmentation of various scenarios.

4.3. Ablation Studies

In this subsection, we validate the impact of each module of our method on three datasets. The hyper-parameters validated on CHASE-DB1 are directly used with STARE.

Effects of Different Prompted Stages: We first explore the effects of inserting the proposed SPM into varied stages of the backbone. As mentioned above, ResNet-101 consists of 4 stages and we treated the head segmenter as the fifth stage. As shown in Table 4, our performance gradually increases as the number of prompted stages increases. More specifically, our method achieves a promising mIoU with five prompted stages on ADE20K. For Vaihingen and CHASE-DB1, the best number of prompted stages is 4, and more prompted stages no longer result in obvious improvements. Thus, we can conclude that more prompted stages are required on large-scale datasets and fewer prompted stages on small/medium-scale datasets.

Table 5. Performance of different recurrent numbers of SPM on three representative datasets.

#Recurrent	ADE20K	Vaihingen	CHASE-DB1
1	40.01	72.60	77.08±0.68
2	41.08	73.10	76.24±0.79
3	41.83	72.24	-

Table 6. Performance of our method with/without semantic-aware prompt learning (SPL) and long-range spatial context modeling (LSCM) on three representative datasets.

Method	ADE20K	Vaihingen	CHASE-DB1
w/o SPL	39.99	71.03	75.88±0.56
w/o LSCM	40.06	72.26	76.45±0.78
Ours	41.83	73.10	77.08±0.68

Effects of Different Recurrent Iterations of SPM: We then explore the recurrent prompt learning mechanism of our SPM. As shown in Table 5, on the ADE20K dataset, our method can obtain better results as the recurrent number R increases, and it achieves the best mIoU 41.83% when R is set to 3. This is because that downstream segmentation tasks on ADE20K have a large domain gap with the pre-trained knowledge from ImageNet, and our SPM needs more recurrent iterations to learn effective prompts progressively. On the Vaihingen dataset, our SPM requires two recurrent iterations to obtain the best results, as the object variances of Vaihingen are smaller than that of ADE20K. On the CHASE-DB1 dataset, with only one iteration, our SPM has a sufficient capacity to generate effective visual prompts and achieve superior performance. Thus we can draw a conclusion that large-scale challenging datasets require more recurrent iterations of prompt learning, while small/medium-scale datasets require fewer iterations.

Effects of Semantic-aware Prompt Learning: In our SPM, interim semantic maps are incorporated to learn visual prompts. Here we ablate this model design by removing the guided semantic information. Specifically, we set all those weights a_i in Eq.5 to 0, making our network learn prompts in a black-box mapping manner. Table 6 (Row 1) shows that removing the semantic-aware information will lead to inferior results on all datasets. For instance, mIoU drops from 41.83% to 39.99% on ADE20K, while Dice decreases from 77.08% to 75.88% on CHASE-DB1. These experiments illustrate that the prior information of interim semantic maps is beneficial for effective prompt learning.

Effects of Long-range Spatial Context Modeling: We further explore the effectiveness of long-range spatial context modeling. Here we implement a variant of SPM that does not explicitly capture long-range context by setting the dilated rate of all convolutional layers in PDC to 1. As shown in Table 6 (Row 2), the mIoU of this variant drops to 40.06% for on ADE20K and 72.26% on Vaihingen,

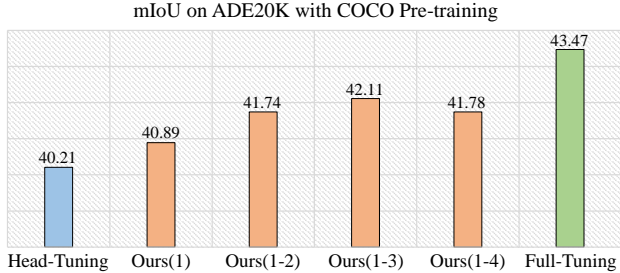


Figure 5. Performance on the ADE20K dataset when the backbone network was pre-trained on the COCO dataset. Ours(i - j) denotes a variant of our method that inserts SPM before stages i - j .

while its Dice decreases to 76.45% on CHASE-DB1. These experiments indicate that the long-range spatial context is meaningful for semantic segmentation prompt learning.

Effects of Different Pre-training Datasets: Finally, we explore the influences of pre-training data from different source domains. Besides the backbone pre-trained on ImageNet, we reimplement our experiments using the ResNet-101 backbone pre-trained on the COCO-Stuff-164K dataset [6], another large-scale semantic segmentation benchmark. Figure 5 summarizes the results of different methods based on the COCO pre-trained backbone. Compared with the results of ImageNet pre-training in Table 4, we observe that our method can achieve a better mIoU of 42.11% by using fewer prompted stages. This phenomenon indicates that it is beneficial to choose models pre-trained on a proper source domain. Nevertheless, many downstream tasks do not have large-scale datasets in practice. Therefore it makes sense to adopt the foundation models pre-trained on ImageNet, since they have good generalization.

4.4. Apply to Transformer

As mentioned above, our method is also generic to the Transformer architecture. Thus in this subsection, we apply the proposed method to fine-tune the large-scale Vision-Transformer (ViT-L) [57], which consists of 24 transformer layers. More specifically, we divide these layers into N stages evenly and perform visual prompt learning before each stage. Meanwhile, we also explore the recurrent mechanism of SPM based on the backbone ViT-L. Following [31], the learning rate multiplier of prompts is set to 10, so that the head segmenter and prompts share the same learning rate. Table 7 summarizes the performance of five variants of our method, which are trained for 160K iterations with a batch size of 8. We can observe that our method achieves a competitive mIoU 45.05% on the ADE20K dataset, when ViT-L is divided into three stages and each SPM performs twice prompt learning. Hence we adopt this setting for ViT-L prompt tuning, which only introduces 1.76M extra prompt parameters.

Based on the ViT-L backbone, we further compare the

Table 7. Ablation Studies of different stage numbers and SPM recurrent numbers of our method on ADK20K when the backbone is the ViT-L pre-trained on ImageNet-21K [44].

#Stage	#Recurrent	#Prompt (M)	mIoU \uparrow
1	1	0.59	42.47
2	1	1.17	44.28
3	1	1.76	44.72
3	2	1.76	45.05
3	3	1.76	44.60

Table 8. Performance of different methods on ADE20K when the backbone is ViT-L pre-trained on ImageNet-21K. Those methods with * are trained with a batch size of 16 and their results are quoted from [31], while other methods are implemented by us with a batch size of 8 due to the limited GPU resources. All methods are optimized for 160K iterations.

Method	Trainable Parameters (M)			mIoU \uparrow
	Backbone	Prompt	Head	
Full-Tuning [2]	304.15	0	13.14	47.53
Head-Tuning [15]	0	0	13.14	37.77
VPT* [31]	0	0.25	13.14	42.11
Bias-Tuning* [53]	0.28	0	13.14	43.40
AdaptFormer [9]	0	3.17	13.14	44.00
VPT+Bias-Tuning*	0.28	2.50	13.14	44.04
Ours	0	1.76	13.14	45.05

proposed method with six stage-of-the-art approaches on ADE20K. As shown in Table 8, our method is much better than VPT [31] that learns ten prompt tokens of each transformer layer. Moreover, with fewer prompt parameters, our method also outperforms the recent AdaptFormer [9] and the ensemble VPT+Bias-Tuning, which learns 100 prompt tokens for each layer and fine-tunes backbone’s bias simultaneously. This is mainly attributed to that our lightweight SPM can generate effective visual prompts using rich information of interim semantic maps. These experiments show the promising potential of our method for large-scale Transformer fine-tuning.

5. Conclusion

In this paper, we propose a universal Stage-wise Prompt-Matched Framework to fine-tune foundation models of CNN/Transformer to handle various downstream tasks. A lightweight Semantic-aware Prompt Matcher is introduced to learn effective visual prompts progressively between different stages of the frozen backbone network, thereby better stimulating pre-trained knowledge and promoting downstream representation learning. We conduct extensive experiments on four datasets of semantic segmentation to verify the performance effectiveness and parameter efficiency of our method. In the future, we would apply the proposed method to more downstream tasks.

Table 9. The top-1 accuracy of different fine-tuning methods for image recognition, when the backbone network is ViT-B pre-trained on ImageNet-21K. We also report the tunable parameter percentage and accuracy gap of various methods relative to *Full-Tuning* in brackets.

Method	Avg Params (M)	CIFAR-100	SVHN	Food-101
Full-Tuning [2]	86.04 (100%)	85.90	97.67	90.09
Head-Tuning [15]	0.07 (0.08%)	69.83 (-16.07)	66.91 (-30.76)	69.74 (-20.35)
VPT [31]	0.08 (0.09%)	82.44 (-3.46)	94.02 (-3.65)	82.98 (-7.11)
AdaptFormer [9]	1.26 (1.46%)	85.90 (+0.00)	96.89 (-0.78)	87.61 (-2.48)
Ours	1.00 (1.16%)	86.62 (+0.72)	97.49 (-0.18)	88.63 (-1.46)

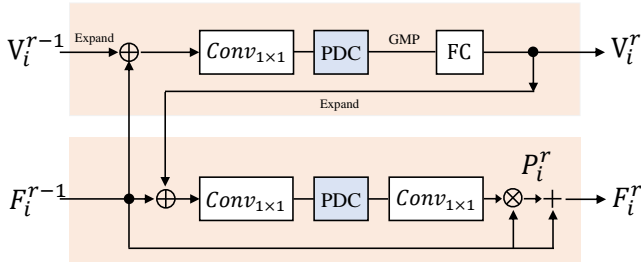


Figure 6. The architecture of Semantic-aware Prompt Matcher for image recognition. Here the interim category probability vector V_i^r is used to learn semantic-aware visual prompts. GMP is a global max-pooling layer, while FC represents a fully-connected layer. "Expand" means that V_i^{r-1} and V_i^r are expanded (via copying) to have the same resolution as F_i^{r-1} before feature concatenation.

Appendix: Apply to Image Recognition

It is worth noting that our method is general to various visual tasks. In this supplementary material, we apply the proposed Stage-wise Prompt-Matched Framework to effectively fine-tune pre-trained foundation models for image recognition. Following the previous work [9], we take ViT-B [57] as the backbone network, which consists of 12 transformer layers and was pre-trained on ImageNet-21K with the self-supervised method MAE [21]. We freeze the parameters of the whole backbone and insert four SPM before layers 1,5,9,12 to hierarchically learn visual prompts. More specifically, as shown in Figure 6, the interim semantic map M_i^{r-1} in our SPM is replaced by the interim category probability vector $V_i^{r-1} \in \mathbb{R}^{C_d}$, where C_d denotes the category number of the downstream image recognition dataset. In the first branch, the expanded V_i^{r-1} and feature F_i^{r-1} are concatenated and fed into a 1×1 convolutional layer, a PDC module, a global max-pooling layer, and a fully-connected layer to generate the refined probability vector V_i^r . The second branch is the same as in the main text. Note that the initial semantic map P_0 is set to the statistic category probability of the training set of the downstream dataset. Here the channel number of our SPM is set to 96 for image recognition. We completely follow the hyper-parameter setting of

AdaptFormer [9] to conduct experiments on three representative datasets, including CIFAR-100 [32], SVHN [18] and Food-101 [4].

The top-1 accuracy of different fine-tuning methods for image recognition is summarized in Table 9. We can observe that the proposed method achieves promising performance on all benchmarks, outperforming the state-of-the-art VPT [31] and AdaptFormer [9] consistently. In particular, our method is also better than *Full-Tuning* [2] on CIFAR-100, and is comparable on SVHN and Food-101. Besides the performance superiority, our method also has great advantages in terms of parameter efficiency. Specifically, our method only need to optimize 1.06M parameter for CIFAR-100/Food-101 and 0.88M parameter for SVHN. On average, the amount of our tunable parameters of our method is 1% of that of *Full-Tuning*. These experiments demonstrate the great potential of our method for image recognition fine-tuning.

References

- [1] 2d semantic labeling - vaihingen data. <https://www.isprs.org/education/benchmarks/UrbanSemLab/2d-sem-label-vaihingen.aspx>. 5
- [2] Pulkit Agrawal, Ross Girshick, and Jitendra Malik. Analyzing the performance of multilayer neural networks for object recognition. In *European conference on computer vision*, pages 329–344. Springer, 2014. 1, 5, 6, 8, 9
- [3] Vijay Badrinarayanan, Alex Kendall, and Roberto Cipolla. Segnet: A deep convolutional encoder-decoder architecture for image segmentation. *IEEE transactions on pattern analysis and machine intelligence*, 39(12):2481–2495, 2017. 1
- [4] Lukas Bossard, Matthieu Guillaumin, and Luc Van Gool. Food-101—mining discriminative components with random forests. In *European conference on computer vision*, pages 446–461. Springer, 2014. 9
- [5] Tom Brown, Benjamin Mann, Nick Ryder, Melanie Subbiah, Jared D Kaplan, Prafulla Dhariwal, Arvind Neelakantan, Pranav Shyam, Girish Sastry, Amanda Askell, et al. Language models are few-shot learners. *Advances in neural information processing systems*, 33:1877–1901, 2020. 2, 7
- [6] Holger Caesar, Jasper Uijlings, and Vittorio Ferrari. Coco-stuff: Thing and stuff classes in context. In *Proceedings of*

- the IEEE conference on computer vision and pattern recognition*, pages 1209–1218, 2018. 8
- [7] Liang-Chieh Chen, George Papandreou, Iasonas Kokkinos, Kevin Murphy, and Alan L Yuille. Semantic image segmentation with deep convolutional nets and fully connected crfs. In *ICLR*, 2015. 2
- [8] Liang-Chieh Chen, George Papandreou, Iasonas Kokkinos, Kevin Murphy, and Alan L Yuille. Deeplab: Semantic image segmentation with deep convolutional nets, atrous convolution, and fully connected crfs. *IEEE transactions on pattern analysis and machine intelligence*, 40(4):834–848, 2017. 2
- [9] Shoufa Chen, Chongjian Ge, Zhan Tong, Jiangliu Wang, Yibing Song, Jue Wang, and Ping Luo. Adaptformer: Adapting vision transformers for scalable visual recognition. *arXiv preprint arXiv:2205.13535*, 2022. 1, 2, 3, 8, 9
- [10] Zhe Chen, Yuchen Duan, Wenhai Wang, Junjun He, Tong Lu, Jifeng Dai, and Yu Qiao. Vision transformer adapter for dense predictions. *arXiv preprint arXiv:2205.08534*, 2022. 2
- [11] MMSegmentation Contributors. MMSegmentation: Openmmlab semantic segmentation toolbox and benchmark. <https://github.com/open-mmlab/mms Segmentation>, 2020. 5
- [12] Jia Deng, Wei Dong, Richard Socher, Li-Jia Li, Kai Li, and Li Fei-Fei. Imagenet: A large-scale hierarchical image database. In *IEEE conference on computer vision and pattern recognition*, pages 248–255. IEEE, 2009. 1, 5
- [13] Jacob Devlin, Ming-Wei Chang, Kenton Lee, and Kristina Toutanova. Bert: Pre-training of deep bidirectional transformers for language understanding. *arXiv preprint arXiv:1810.04805*, 2018. 2
- [14] Henghui Ding, Xudong Jiang, Bing Shuai, Ai Qun Liu, and Gang Wang. Semantic correlation promoted shape-variant context for segmentation. In *Proceedings of the IEEE/CVF Conference on Computer Vision and Pattern Recognition*, pages 8885–8894, 2019. 1
- [15] Jeff Donahue, Yangqing Jia, Oriol Vinyals, Judy Hoffman, Ning Zhang, Eric Tzeng, and Trevor Darrell. Decaf: A deep convolutional activation feature for generic visual recognition. In *International conference on machine learning*, pages 647–655. PMLR, 2014. 1, 5, 6, 8, 9
- [16] Alexey Dosovitskiy, Lucas Beyer, Alexander Kolesnikov, Dirk Weissenborn, Xiaohua Zhai, Thomas Unterthiner, Mostafa Dehghani, Matthias Minderer, Georg Heigold, Sylvain Gelly, et al. An image is worth 16x16 words: Transformers for image recognition at scale. *arXiv preprint arXiv:2010.11929*, 2020. 2, 3
- [17] Muhammad Moazam Fraz, Paolo Remagnino, Andreas Hoppe, Bunyarit Uyyanonvara, Alicja R Rudnicka, Christopher G Owen, and Sarah A Barman. An ensemble classification-based approach applied to retinal blood vessel segmentation. *IEEE Transactions on Biomedical Engineering*, 59(9):2538–2548, 2012. 5
- [18] Ian J Goodfellow, Yaroslav Bulatov, Julian Ibarz, Sacha Arnoud, and Vinay Shet. Multi-digit number recognition from street view imagery using deep convolutional neural networks. *arXiv preprint arXiv:1312.6082*, 2013. 9
- [19] Jiaqi Gu, Hyoukjun Kwon, Dilin Wang, Wei Ye, Meng Li, Yu-Hsin Chen, Liangzhen Lai, Vikas Chandra, and David Z Pan. Multi-scale high-resolution vision transformer for semantic segmentation. In *Proceedings of the IEEE/CVF Conference on Computer Vision and Pattern Recognition*, pages 12094–12103, 2022. 1
- [20] Junjun He, Zhongying Deng, Lei Zhou, Yali Wang, and Yu Qiao. Adaptive pyramid context network for semantic segmentation. In *IEEE Conference on Computer Vision and Pattern Recognition*, pages 7519–7528, 2019. 4
- [21] Kaiming He, Xinlei Chen, Saining Xie, Yanghao Li, Piotr Dollár, and Ross Girshick. Masked autoencoders are scalable vision learners. In *Proceedings of the IEEE/CVF Conference on Computer Vision and Pattern Recognition*, pages 16000–16009, 2022. 9
- [22] Kaiming He, Xiangyu Zhang, Shaoqing Ren, and Jian Sun. Deep residual learning for image recognition. In *Proceedings of the IEEE conference on computer vision and pattern recognition*, pages 770–778, 2016. 2, 5
- [23] Xiang He, Sibe Yang, Guanbin Li, Haofeng Li, Huiyou Chang, and Yizhou Yu. Non-local context encoder: Robust biomedical image segmentation against adversarial attacks. In *Proceedings of the AAAI Conference on Artificial Intelligence*, volume 33, pages 8417–8424, 2019. 1
- [24] AD Hoover, Valentina Kouznetsova, and Michael Goldbaum. Locating blood vessels in retinal images by piecewise threshold probing of a matched filter response. *IEEE Transactions on Medical Imaging*, 19(3):203–210, 2000. 5
- [25] Neil Houlsby, Andrei Giurgiu, Stanislaw Jastrzebski, Bruna Morrone, Quentin De Laroussilhe, Andrea Gesmundo, Mona Attariyan, and Sylvain Gelly. Parameter-efficient transfer learning for nlp. In *International Conference on Machine Learning*, pages 2790–2799. PMLR, 2019. 5, 6
- [26] Hanzhe Hu, Jinshi Cui, and Liwei Wang. Region-aware contrastive learning for semantic segmentation. In *Proceedings of the IEEE/CVF International Conference on Computer Vision*, pages 16291–16301, 2021. 2
- [27] Shengding Hu, Ning Ding, Huadong Wang, Zhiyuan Liu, Jingang Wang, Juanzi Li, Wei Wu, and Maosong Sun. Knowledgeable prompt-tuning: Incorporating knowledge into prompt verbalizer for text classification. In *Proceedings of the Annual Meeting of the Association for Computational Linguistics*, pages 2225–2240, 2022. 2
- [28] Zilong Huang, Xinggang Wang, Lichao Huang, Chang Huang, Yunchao Wei, and Wenyu Liu. Ccnet: Criss-cross attention for semantic segmentation. In *Proceedings of the IEEE/CVF international conference on computer vision*, pages 603–612, 2019. 2
- [29] Zilong Huang, Yunchao Wei, Xinggang Wang, Wenyu Liu, Thomas S Huang, and Humphrey Shi. Alignseg: Feature-aligned segmentation networks. *IEEE Transactions on Pattern Analysis and Machine Intelligence*, 44(1):550–557, 2021. 1
- [30] Chao Jia, Yinfei Yang, Ye Xia, Yi-Ting Chen, Zarana Parekh, Hieu Pham, Quoc Le, Yun-Hsuan Sung, Zhen Li, and Tom Duerig. Scaling up visual and vision-language representation learning with noisy text supervision. In *International*

- Conference on Machine Learning*, pages 4904–4916. PMLR, 2021. 2
- [31] Menglin Jia, Luming Tang, Bor-Chun Chen, Claire Cardie, Serge Belongie, Bharath Hariharan, and Ser-Nam Lim. Visual prompt tuning. *arXiv preprint arXiv:2203.12119*, 2022. 1, 2, 3, 8, 9
- [32] Alex Krizhevsky, Geoffrey Hinton, et al. Learning multiple layers of features from tiny images. 2009. 9
- [33] Liulei Li, Tianfei Zhou, Wenguan Wang, Jianwu Li, and Yi Yang. Deep hierarchical semantic segmentation. In *Proceedings of the IEEE/CVF Conference on Computer Vision and Pattern Recognition*, pages 1246–1257, 2022. 2
- [34] Xiangtai Li, Ansheng You, Zhen Zhu, Houlong Zhao, Maoke Yang, Kuiyuan Yang, Shaohua Tan, and Yunhai Tong. Semantic flow for fast and accurate scene parsing. In *European Conference on Computer Vision*, pages 775–793. Springer, 2020. 1
- [35] Di Lin, Yuanfeng Ji, Dani Lischinski, Daniel Cohen-Or, and Hui Huang. Multi-scale context intertwining for semantic segmentation. In *Proceedings of the European Conference on Computer Vision (ECCV)*, pages 603–619, 2018. 2
- [36] Zachary C Lipton, John Berkowitz, and Charles Elkan. A critical review of recurrent neural networks for sequence learning. *arXiv preprint arXiv:1506.00019*, 2015. 4
- [37] Lingbo Liu, Zewei Yang, Guanbin Li, Kuo Wang, Tianshui Chen, and Liang Lin. Aerial images meet crowdsourced trajectories: a new approach to robust road extraction. *IEEE transactions on neural networks and learning systems*, 2022. 1
- [38] Pengfei Liu, Weizhe Yuan, Jinlan Fu, Zhengbao Jiang, Hiroaki Hayashi, and Graham Neubig. Pre-train, prompt, and predict: A systematic survey of prompting methods in natural language processing. *arXiv preprint arXiv:2107.13586*, 2021. 1, 3
- [39] Shu Liu, Lu Qi, Haifang Qin, Jianping Shi, and Jiaya Jia. Path aggregation network for instance segmentation. In *Proceedings of the IEEE conference on computer vision and pattern recognition*, pages 8759–8768, 2018. 1
- [40] Jonathan Long, Evan Shelhamer, and Trevor Darrell. Fully convolutional networks for semantic segmentation. In *Proceedings of the IEEE conference on computer vision and pattern recognition*, pages 3431–3440, 2015. 1, 2
- [41] Yufei Ma, Minkyu Kim, Yu Cao, Sarma Vrudhula, and Jaesun Seo. End-to-end scalable fpga accelerator for deep residual networks. In *IEEE International Symposium on Circuits and Systems*, pages 1–4. IEEE, 2017. 2
- [42] Shervin Minaee, Yuri Y Boykov, Fatih Porikli, Antonio J Plaza, Nasser Kehtarnavaz, and Demetri Terzopoulos. Image segmentation using deep learning: A survey. *IEEE transactions on pattern analysis and machine intelligence*, 2021. 1
- [43] Alec Radford, Jong Wook Kim, Chris Hallacy, Aditya Ramesh, Gabriel Goh, Sandhini Agarwal, Girish Sastry, Amanda Askell, Pamela Mishkin, Jack Clark, et al. Learning transferable visual models from natural language supervision. In *International Conference on Machine Learning*, pages 8748–8763. PMLR, 2021. 2
- [44] Tal Ridnik, Emanuel Ben-Baruch, Asaf Noy, and Lihi Zelnik-Manor. Imagenet-21k pretraining for the masses. *arXiv preprint arXiv:2104.10972*, 2021. 8
- [45] Olaf Ronneberger, Philipp Fischer, and Thomas Brox. U-net: Convolutional networks for biomedical image segmentation. In *International Conference on Medical image computing and computer-assisted intervention*, pages 234–241. Springer, 2015. 2
- [46] Robin Strudel, Ricardo Garcia, Ivan Laptev, and Cordelia Schmid. Segmenter: Transformer for semantic segmentation. In *Proceedings of the IEEE/CVF International Conference on Computer Vision*, pages 7262–7272, 2021. 1, 2
- [47] Zhixing Tan, Xiangwen Zhang, Shuo Wang, and Yang Liu. Msp: Multi-stage prompting for making pre-trained language models better translators. In *Proceedings of the 60th Annual Meeting of the Association for Computational Linguistics (Volume 1: Long Papers)*, pages 6131–6142, 2022. 2
- [48] Ashish Vaswani, Noam Shazeer, Niki Parmar, Jakob Uszkoreit, Llion Jones, Aidan N Gomez, Łukasz Kaiser, and Illia Polosukhin. Attention is all you need. *Advances in neural information processing systems*, 30, 2017. 2
- [49] Yang Wang, Yubin Qin, Dazheng Deng, Jingchuan Wei, Yang Zhou, Yuanqi Fan, Tianbao Chen, Hao Sun, Leibo Liu, Shaojun Wei, et al. A 28nm 27.5 tops/w approximate-computing-based transformer processor with asymptotic sparsity speculating and out-of-order computing. In *IEEE International Solid-State Circuits Conference*, volume 65, pages 1–3. IEEE, 2022. 2
- [50] Enze Xie, Wenhai Wang, Zhiding Yu, Anima Anandkumar, Jose M Alvarez, and Ping Luo. Segformer: Simple and efficient design for semantic segmentation with transformers. *Advances in Neural Information Processing Systems*, 34:12077–12090, 2021. 1
- [51] Zhengyuan Yang, Zhe Gan, Jianfeng Wang, Xiaowei Hu, Yumao Lu, Zicheng Liu, and Lijuan Wang. An empirical study of gpt-3 for few-shot knowledge-based vqa. In *Proceedings of the AAAI Conference on Artificial Intelligence*, volume 36, pages 3081–3089, 2022. 2
- [52] Changqian Yu, Jingbo Wang, Chao Peng, Changxin Gao, Gang Yu, and Nong Sang. Learning a discriminative feature network for semantic segmentation. In *Proceedings of the IEEE conference on computer vision and pattern recognition*, pages 1857–1866, 2018. 1
- [53] Elad Ben Zaken, Shauli Ravfogel, and Yoav Goldberg. Bitfit: Simple parameter-efficient fine-tuning for transformer-based masked language-models. *arXiv preprint arXiv:2106.10199*, 2021. 5, 6, 8
- [54] Wei Zeng, Xiaozhe Ren, Teng Su, Hui Wang, Yi Liao, Zhiwei Wang, Xin Jiang, ZhenZhang Yang, Kaisheng Wang, Xiaoda Zhang, et al. Pangu- α : Large-scale autoregressive pretrained chinese language models with auto-parallel computation. *arXiv preprint arXiv:2104.12369*, 2021. 2, 7
- [55] Jeffrey O Zhang, Alexander Sax, Amir Zamir, Leonidas Guibas, and Jitendra Malik. Side-tuning: a baseline for network adaptation via additive side networks. In *European Conference on Computer Vision*, pages 698–714. Springer, 2020. 5, 6

- [56] Hengshuang Zhao, Jianping Shi, Xiaojuan Qi, Xiaogang Wang, and Jiaya Jia. Pyramid scene parsing network. In *IEEE conference on computer vision and pattern recognition*, pages 2881–2890, 2017. [2](#), [5](#)
- [57] Sixiao Zheng, Jiachen Lu, Hengshuang Zhao, Xiatian Zhu, Zekun Luo, Yabiao Wang, Yanwei Fu, Jianfeng Feng, Tao Xiang, Philip HS Torr, et al. Rethinking semantic segmentation from a sequence-to-sequence perspective with transformers. In *Proceedings of the IEEE/CVF conference on computer vision and pattern recognition*, pages 6881–6890, 2021. [5](#), [8](#), [9](#)
- [58] Zilong Zhong, Zhong Qiu Lin, Rene Bidart, Xiaodan Hu, Ibrahim Ben Daya, Zhifeng Li, Wei-Shi Zheng, Jonathan Li, and Alexander Wong. Squeeze-and-attention networks for semantic segmentation. In *Proceedings of the IEEE/CVF conference on computer vision and pattern recognition*, pages 13065–13074, 2020. [2](#)
- [59] Bolei Zhou, Hang Zhao, Xavier Puig, Sanja Fidler, Adela Barriuso, and Antonio Torralba. Scene parsing through ade20k dataset. In *Proceedings of the IEEE conference on computer vision and pattern recognition*, pages 633–641, 2017. [5](#)
- [60] Rui Zhu, Shifeng Zhang, Xiaobo Wang, Longyin Wen, Hailin Shi, Liefeng Bo, and Tao Mei. Scratchdet: Training single-shot object detectors from scratch. In *Proceedings of the IEEE/CVF Conference on Computer Vision and Pattern Recognition*, pages 2268–2277, 2019. [1](#), [5](#), [6](#)
- [61] Zhen Zhu, Mengde Xu, Song Bai, Tengpeng Huang, and Xi-ang Bai. Asymmetric non-local neural networks for semantic segmentation. In *IEEE International Conference on Computer Vision*, pages 593–602, 2019. [4](#)